SUPPLEMENT

Figure 1. Single flash ERG responses of increasing intensity for WT and Rho+/- mice in light-adapted conditions. Serial responses to increasing flash stimuli obtained from WT and Rho+/- mice in light-adapted conditions for selected intensities (**A**) and plotted as a function a-wave and b-wave versus light intensities (**B**). Responses in light-adapted conditions are examined after bleaching at 1.4 log cd s m^{-2} for 15 min.

Figure 2. TEM of negatively stained native discs isolated from Rho+/- mice. A. Morphology of a native disc. **B**. Average of eight power spectra calculated from regions on the displayed disc, e.g., area marked by the broken circle (1). Powder diffraction is evident, indicating paracrystallinity of Rho. **C**. Average of eight power spectra calculated from regions on the carbon film, e.g., area marked by the broken circle (2). No powder diffraction is evident. Scale bars: 250 nm (**A**) and $(4\ nm)^{-1}$ (**B** and **C**). Isolated discs were adsorbed to glow discharged carbon support films mounted on electron microscopy grids and negatively stained with 0.5% uranyl acetate. Electron micrographs of disc membranes were recorded with a Hitachi H-7000 electron microscope operated at 100 kV. Single power spectra of electron micrographs and averages of several power spectra were calculated with the SEMPER image processing system (1).

Figure 3. Rho oligomer in paracrystal. View from the cytoplasmic (A) and extracellular (B) side. Single dimers are marked by ellipses. Phospholipids (green and red) are flowing between double Rho rows (black arrows on A) and between rows of dimers at the extracellular side (black arrows on B). A molecular model of the Rho oligomer was constructed using the refined crystal structure of Rho (2,3) (Protein Data Bank (PDB) entry 1HZX). The carbohydrate moieties connected to Asn-2 and Asn-15, as well as all ions, detergents, water, and additive molecules, were removed. The missing amino acids 236–240 and 331–333 were inserted using the Homology module from the InsightII package and were subsequently optimized with the Discovery module (InsightII 2000, Accelrys Inc.). All titratable groups in the protein were considered to be charged. Based on the AFM measurements (4-6) of Rho in the paracrystal, a model was constructed where helices H-IV and H-V form an interface between Rho monomers.

Energetic considerations together with geometrical constraints obtained from AFM excluded other models as oligomeric structures. Oligomers in our model (1N3M entry in PDB) were built from separate dimers and linked together by a long loop between H-V and H-VI. The dimer is a repetitive motif in the oligomer, thus tetramers and higher structures were connected in the same manner as dimers.

Membrane embedding. The protein was embedded in the three-component lipid bilayer found in rod discs, composed of phospholipids with phosphatidylcholine headgroups (PC) on the intradiscal side and phosphatidylethanolamine (PE) together with phosphatidylserine (PS) headgroups (three times more PE headgroups than PS) on the cytoplasmic side (7,8). All three types of phospholipids contained the saturated stearoyl chain (18:0) in the *sn*1 position and the polyunsaturated docosahexaenoyl chain (22:6) in the *sn*2 position. The lipid bilayer had a thickness of 38 Å (defined as the distance between the planes formed by the phosphorus atoms of the two leaflets). The position of the protein in the membrane was fitted considering the intrinsic hydrophobic surface of the protein and the two palmitoyl moieties connected to Cys^{322} and Cys^{323}. The model contained 21 PC, 17 PE, and 5 PS molecules per two Rho molecules in a periodic cell. Dimensions and angles of the periodic cell were derived from AFM measurements: edges 3.8 nm and 8.4 nm with angle 85º between them. The number of phospholipids was determined experimentally by molecular dynamics based on the stability of the system.

Solvation. The protein-lipid system was solvated in a water bath with a Solvate package of VMD (9). TIP3P-type water molecules were used as a default in VMD. Extension of the periodic box along the z-dimension (perpendicular to the membrane) was determined by adding 1 nm of free space to the vertical dimension of Rho on both sides. Altogether, the system contained ~4,000 water molecules in the periodic cell. Ionization procedures were also conducted in VMD to neutralize the system and achieve an ionic strength of 0.05 M. Charge neutralization was essential for the particle mesh Ewald (PME) procedure (10) used in molecular dynamics. The size of the entire system was about 30,000 atoms.

Molecular dynamics simulations. All simulations were performed using the NAMD2 program (11). The necessary structure topology files were taken from the All-Hydrogen Force Field CHARMM27 (12-16). For protonated retinal Schiff base parameters we used data derived for bacteriorhodopsin (17-19). All simulations were performed with full electrostatics calculations (PME procedure) and periodic boundary conditions with a rhombic unit cell of 3.8 x 8.4 x 9.8 nm and 85º x 90º x 90º. After insertion of phospholipids between Rho monomers, solvation, and ionization, the energy of the system was minimized, with the Rho monomers frozen in their initial positions. Next, the system was simulated at a constant temperature of 300 K for 50 ps, using the same constraints. This procedure allowed lipids to adjust around the protein and water to diffuse into crevices of the protein and hydrophilic parts of the membrane. Then all systems were allowed to move for 50 ps while dimensions of the periodic box were fixed, as in the previous simulations. The entire system was then simulated with a flexible cell for 500 ps of molecular dynamics. In all simulations the NPT ensemble was used with a constant pressure of 1013 hPa and a temperature of 300 K. Langevin dynamics were used to control fluctuations in pressure and temperature. The periodic box was subjected to anisotropic cell fluctuations to allow changing of each box dimension independently. A membrane of the same composition as used with Rho was simulated separately in a periodic box to calculate the density of phospholipids and investigate the stability of such a membrane. The simulation was performed at a constant temperature of 300 K and a constant pressure of 1013 hPa for 500 ps.

Figure 4. Rho oligomer without cytoplasmic loops seen from the cytoplasmic side. One dimer is marked by the ellipse. Positions of phosphorus atoms of phospholipids are marked by spheres: red – PE, green – PS. PS are grouped at the interface between dimers (as indicated by arrows) because of the high number of positively charged residues there. Theoretical calculation of lipids and Rho at different ratios may allow visualizations of the impact of increased lipid amounts on the Rho density. Molecular dynamics of a solvated lipid bilayer composed of PC on one side and PE/PS on the other side revealed that such a membrane is stable, while the membranes composed only of PC and PE were unstable. The large hydrophilic choline headgroup of PC molecules interact with their

neighbors to form stable networks by ionic interactions. This surface is therefore flat with strong surface tension. In ethanolamine groups a charge is concentrated within a much smaller area, and PE phospholipids prefer to form long rows instead of 2D networks. This leads to segregation of the phospholipids with emerging lipid domains. During simulation, adjacent rows separated to form a rough surface, with some rows located higher or lower than the surface mean. Addition of PS improved this situation because the serine headgroups are larger and more charged, allowing the formation of branched networks. A ratio of one PS molecule to 3 PE was sufficient to prevent formation of separated rows or domains.

Simulations performed for Rho oligomers in the membrane were performed in a rhombic periodic box with dimensions 3.8 x 8.4 x 9.8 nm and angles 85º x 90º x 90º. In this unit cell 21 PC, 17 PE, and 5 PS molecules could fit between Rho molecules located as in the 1N3M model. A cytoplasmic view of the investigated system is depicted in Figure 8A. Rho molecules are located in double rows running vertically; one dimer from such a row is indicated by an ellipse in the figure. The main streams of phospholipids are present on both sides of the double rows. After removal of the cytoplasmic loops of Rho molecules, additional space accessible to phospholipids becomes visible (Figure 2, supplement). In contrast to the cytoplasmic side, there are phospholipids present between Rho dimers at the extracellular (intradiscal) side (Figure 8B). The double row structure of Rho dimers running vertically is invisible here.

Figure 5. Rho dimer (side view). Phospholipids are drawn in sticks and phosphorus atoms are marked by spheres in the colors of the corresponding phospholipid head, i.e., red – ethanolamine (PE), green – serine (PS), purple – choline (PC). Carbon atoms in PC phospholipids are in gray. Figure 3, supplement shows a side view of a Rho dimer with a part of the membrane bilayer. Only a small number of phospholipids are present at the dimer-dimer interface. Phosphorus atoms at the cytoplasmic side in this interface are positioned lower than adjacent phospholipids located between double rows of Rho (left and right sides). This structure is formed because the cytoplasmic loops of the Rho molecules are spread over the cytoplasmic side of the membrane, covering the phospholipids (Figure 3, supplement). How will the density of Rho impact its interactions

with partner proteins? We modeled monomeric Rho in the phospholipids bilayer at 126, 95, and 62 ratios of phospholipids/Rho. Note that the chemical analysis of the phospholipid and Rho contents in mouse, rat, and bovine ROS revealed a ratio of 54-86 phospholipids/Rho (20,21). First, for the 126 phospholipids/monomeric Rho, an average distance between two freely diffusing neighboring Rho molecules was ~7.0 nm, and at the cytoplasmic side the protein-free space was ~3.0 nm. The arrestin interaction area formed a rectangular area 8.5 nm long and 3.5 nm wide (at broadest side) and 2.0 nm wide (at narrowest side); thus, arrestin covered more than half of both Rho molecules. G protein extends 5.5 nm (22), assuming N-terminal helix in the membrane plane (22), a distance that is less than the lipid-free space between two Rho molecules. In the second case of 95 phospholipids/Rho, on the cytoplasmic side the protein-free space is reduced to only ~2.5 nm. Finally, in the case of 62 phospholipids/Rho, on the cytoplasmic side the protein-free space is reduced to ~1.4 nm. Thus, in all cases, even if the amount of phospholipids were increased above normal concentration, arrestin and Gtα would bridge adjacent Rho molecules. An increased number of phospholipids would increase the spacing between monomeric Rho so minimally that any advantage of faster diffusion or a less crowded interaction with partner proteins would be negligible.

REFERENCES FOR THE SUPPLEMENT

1. Saxton, W. O. (1996) *J Struct Biol* **116**, 230-236
2. Palczewski, K., Kumasaka, T., Hori, T., Behnke, C. A., Motoshima, H., Fox, B. A., Le Trong, I., Teller, D. C., Okada, T., Stenkamp, R. E., Yamamoto, M., and Miyano, M. (2000) *Science* **289**, 739-745
3. Teller, D. C., Okada, T., Behnke, C. A., Palczewski, K., and Stenkamp, R. E. (2001) *Biochemistry* **40**, 7761-7772
4. Liang, Y., Fotiadis, D., Filipek, S., Saperstein, D. A., Palczewski, K., and Engel, A. (2003) *J Biol Chem* **278**, 21655-21662
5. Fotiadis, D., Liang, Y., Filipek, S., Saperstein, D. A., Engel, A., and Palczewski, K. (2003) *Nature* **421**, 127-128
6. Fotiadis, D., Liang, Y., Filipek, S., Saperstein, D. A., Engel, A., and Palczewski, K. (2004) *FEBS Lett* **564**, 281-288

7. Giusto, N. M., Pasquare, S. J., Salvador, G. A., Castagnet, P. I., Roque, M. E., and Ilincheta de Boschero, M. G. (2000) *Prog Lipid Res* **39**, 315-391
8. Saiz, L., and Klein, M. L. (2001) *Biophys J* **81**, 204-216
9. Humphrey, W., Dalke, A., and Schulten, K. (1996) *J Mol Graph* **14**, 33-38, 27-38
10. Darden, T., York, D., and Pedersen, L. (1993) *J Chem Phys* **98**, 10089-10092
11. Kale, L., Skeel, R., Bhandarkar, M., Brunner, R., Gursoy, A., Krawetz, N., Phillips, J., Shinozaki, A., Varadarajan, K., and Schulten, K. (1999) *J Comp Phys* **151**, 283-312
12. MacKerell, J., A. D., Bashford, D., Bellott, M., Dunbrack Jr., R. L., Evanseck, J. D., Field, M. J., Fischer, S., Gao, J., Guo, H., Ha, S., Joseph-McCarthy, D., Kuchnir, L., Kuczera, K., Lau, F. T. K., Mattos, C., Michnick, S., Ngo, T., Nguyen, D. T., Prodhom, B., Reiher, I., W.E., Roux, B., Schlenkrich, M., Smith, J. C., Stote, R., Straub, J., Watanabe, M., Wiorkiewicz-Kuczera, J., Yin, D., and Karplus, M. (1998) *J Phys Chem B* **102**, 3586-3616
13. Feller, S. E., Yin, D., Pastor, R. W., and MacKerell, A. D., Jr. (1997) *Biophys J* **73**, 2269-2279
14. Schlenkrich, M., Brickmann, J., MacKerell, J., A.D., and Karplus, M. (1996) *Empirical Potential Energy Function for Phospholipids: Criteria for Parameter Optimization and Applications*. Biological membranes: A molecular perspective from computation and experiment (K.M. Merz and B. Roux, E., Ed.), Birkhauser, Boston
15. Yin, D., and MacKerell, J. A. D. (1998) *J Comp Chem*, 334-338
16. MacKerell, J., A.D. (1997) *J Chim Phys* **94**, 1436-1447
17. Tajkhorshid, E., Baudry, J., Schulten, K., and Suhai, S. (2000) *Biophys J* **78**, 683-693
18. Tajkhorshid, E., and Suhai, S. (1999) *J Phys Chem B* **103**, 5581-5590
19. Tajkhorshid, E., Paizs, B., and Suhai, S. (1997) *J Phys Chem B* **101**, 8021-8028
20. Stone, W. L., Farnsworth, C. C., and Dratz, E. A. (1979) *Exp Eye Res* **28**, 387-397
21. Calvert, P. D., Govardovskii, V. I., Krasnoperova, N., Anderson, R. E., Lem, J., and Makino, C. L. (2001) *Nature* **411**, 90-94
22. Zhang, Z., Melia, T. J., He, F., Yuan, C., McGough, A., Schmid, M. F., and Wensel, T. G. (2004) *J Biol Chem*, (in press)

Supplement

Figure 1
supplement

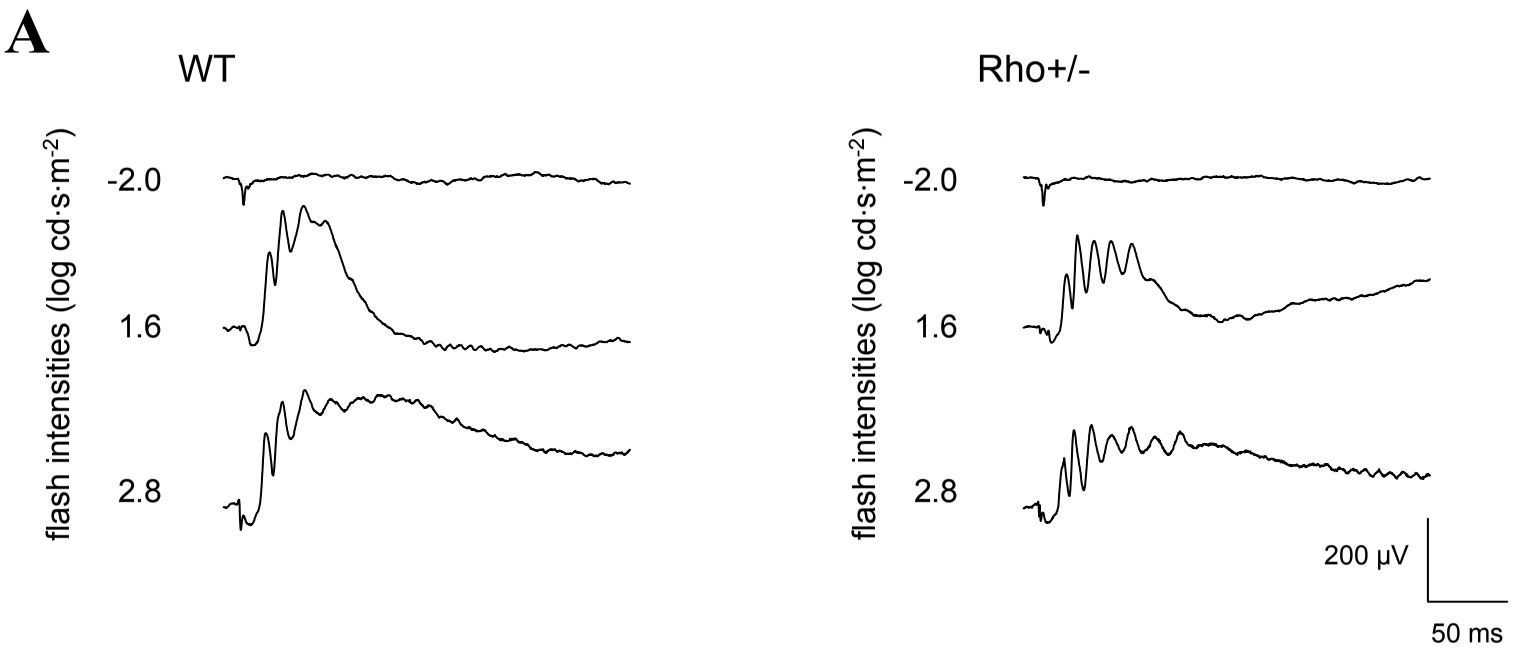

Figure 1
supplement

B

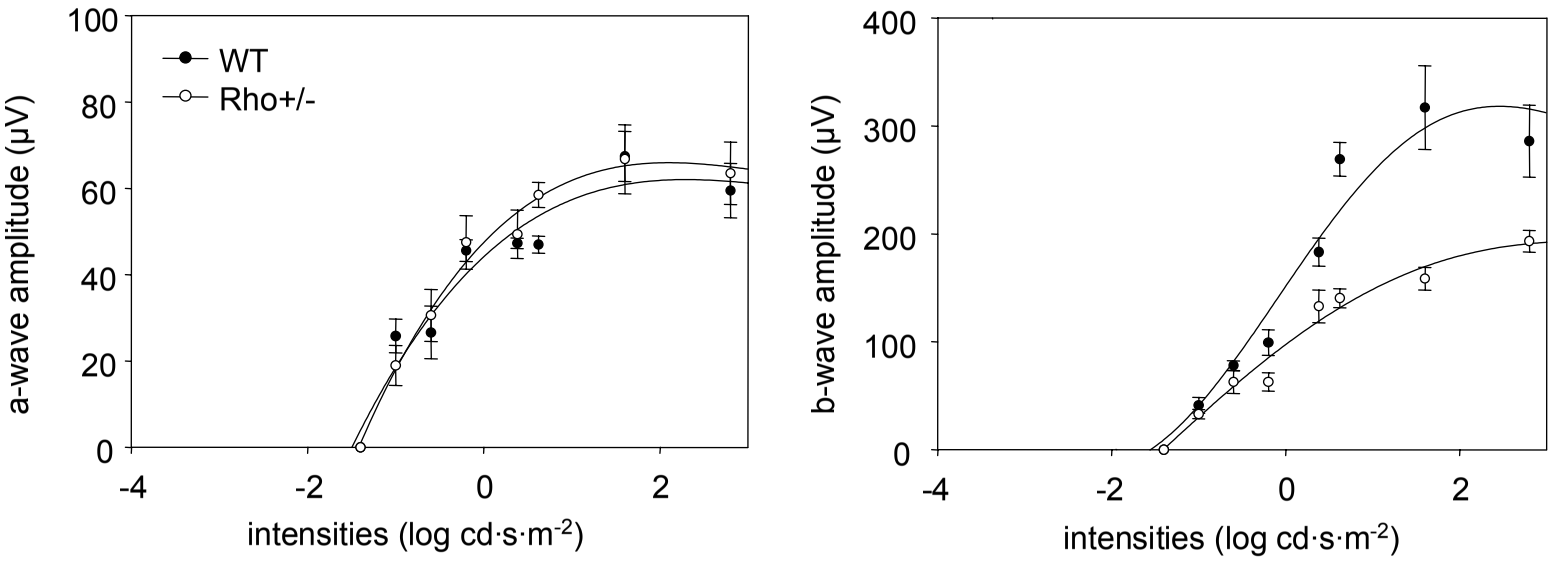

Figure 2
supplement

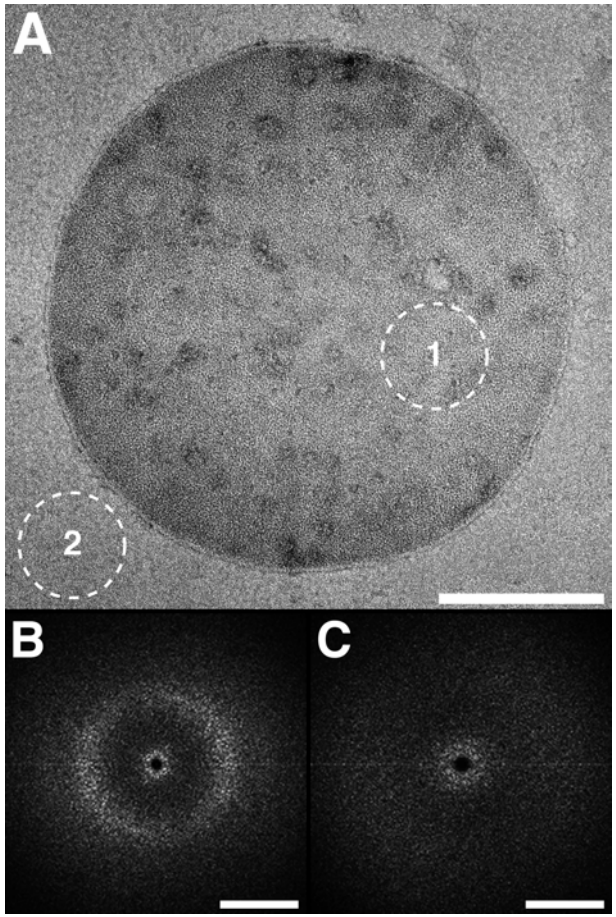

Figure 3
supplement

A

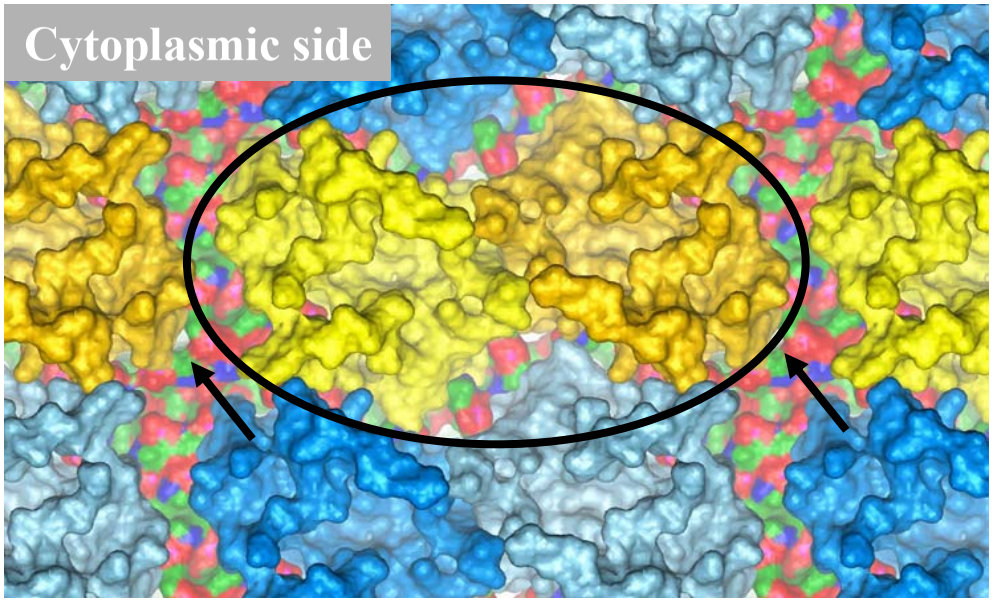

B

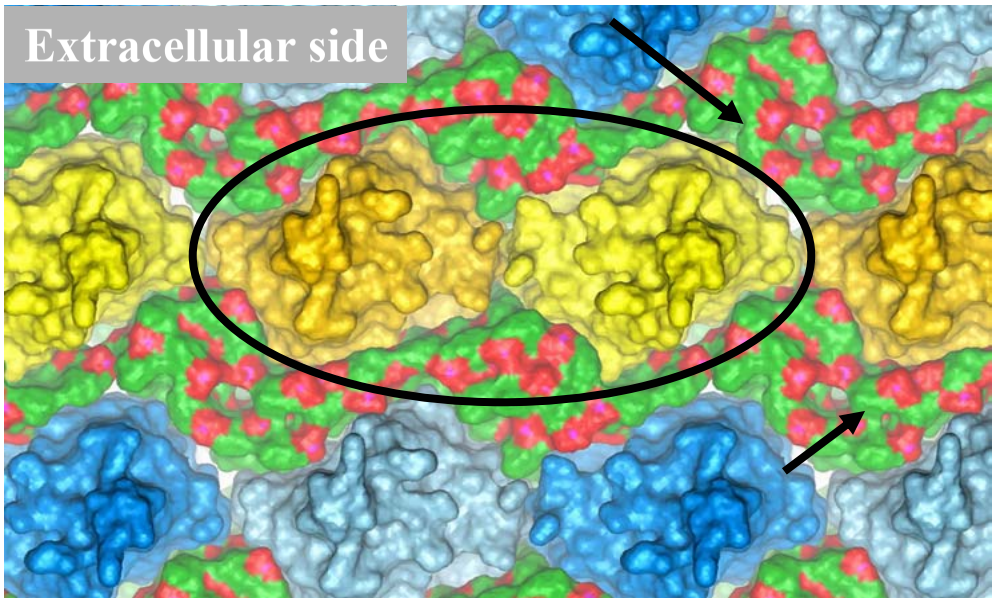

Figure 4
supplement

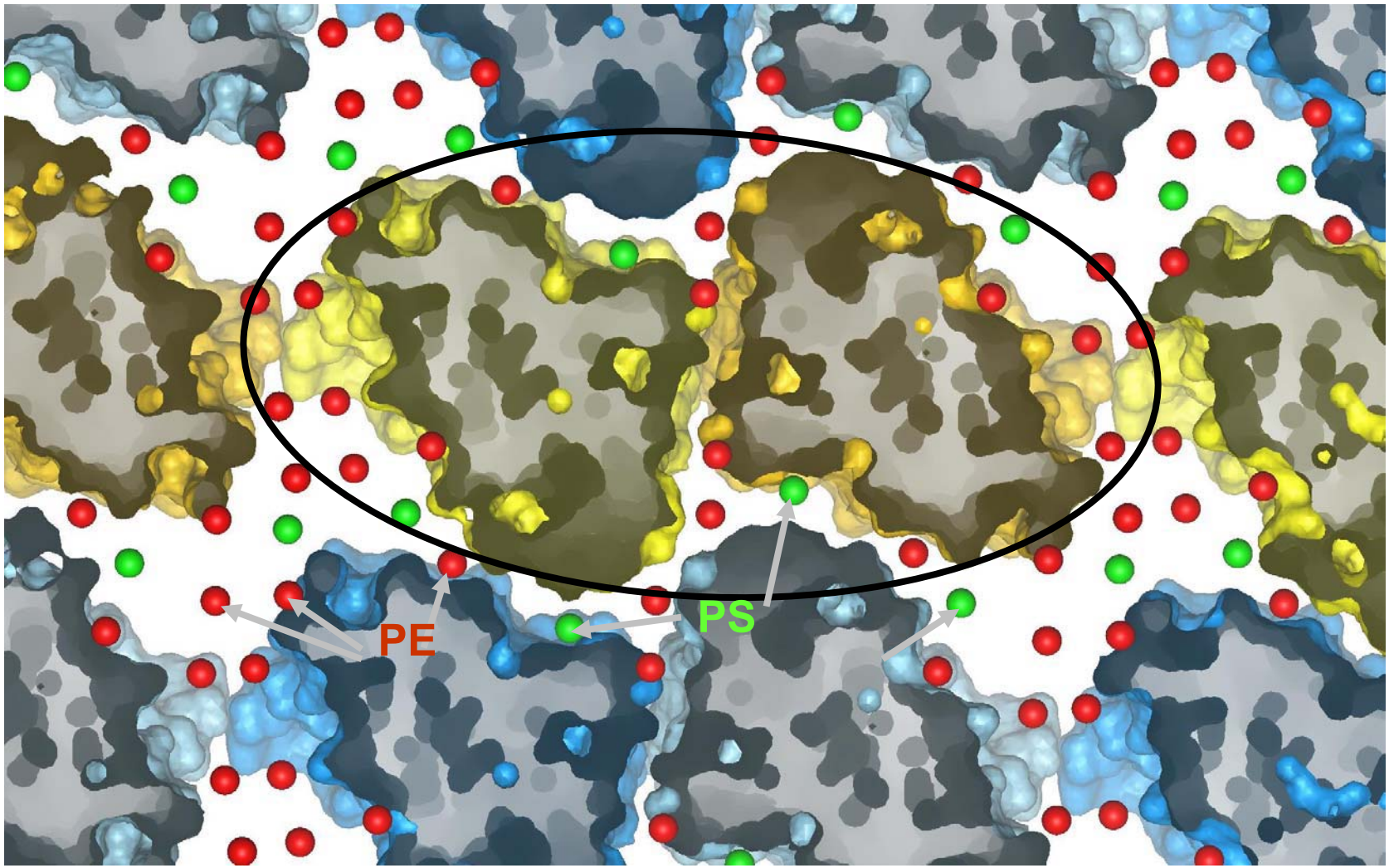

Figure 5
supplement